Materials Science & Engineering A 639 (2015) 114–121

Contents lists available at ScienceDirect

Materials Science & Engineering A

journal homepage: www.elsevier.com/locate/msea

Effects of minor Si on microstructures and room temperature fracture toughness of niobium solid solution alloys

Bin Kong, Lina Jia, Linfen Su, Kai Guan, Junfei Weng, Hu Zhang*

Key Laboratory of Aerospace Materials and Performance, Ministry of Education, School of Materials Science and Engineering, Beihang University, Beijing 100191, China

ARTICLE INFO

Article history:
Received 4 February 2015
Received in revised form
27 April 2015
Accepted 28 April 2015
Available online 8 May 2015

Keywords:
Niobium solid solution alloys
Minor Si
Heat treatment
Microstructure
Room temperature fracture toughness.

ABSTRACT

Controlling the elements content in the niobium solid solution (Nb_{SS}) is significant for the better comprehensive performance of Nb-silicide-based alloys. In this paper, the effects of minor Si on the microstructures and room temperature fracture toughness of Nb–(0/0.5/1/2)Si–27.63Ti–12.92Cr–2.07Al–1.12Hf (at%, unless stated otherwise) solid solution alloys were investigated. The alloys were processed by vacuum arc-casting (AC), and then heat treated (HT) at 1425 °C for 10 h. In HT alloys, Nb_{SS} grains are refined gradually with the increase of Si content. Meanwhile, the volume fraction of Cr_2Nb and silicides phases precipitates increases. The fracture toughness of HT alloys decreases at first but then increases in the range of 0 to 2% Si, because it is a combinatorial process of positive and negative effects caused by the addition of Si. The refinement of Nb_{SS} grains displays positive effect on fracture toughness, while the increase of solid solubility of Si in Nb_{SS} and brittle Cr_2Nb and Nb-silicides precipitate phases display negative effect.

1. Introduction

The desire for more efficient engine performance has necessitated research for advanced materials. Nb-silicide-based alloys, which possess high melting point, low density and excellent high temperature strength, are promising candidates for future high-temperature turbine-engine applications [1–5]. In Nb-silicide-based alloys, niobium solid solution (Nb_{SS}) phase plays an important role in enhancing room temperature fracture toughness; on the other hand, intermetallic phases (Nb_5Si_3, Nb_3Si, and Cr_2Nb) possess good high temperature strength and oxidation resistance but poor fracture toughness [5–8]. Therefore, improving the properties of Nb_{SS} is significant for further development of the performance of Nb-silicide-based alloys.

With body-centered cubic (b.c.c) lattice structure, Nb could form a continuous series of solid solutions with Ti, W, Mo, Ta, and V, and limited solid solutions with Cr, Al, Hf and Zr. According to the study of Begley et al. [9], alloying additions such as W, Mo, V, Cr, Al, and Zr raised the brittle-to-ductile transition temperature (BDTT) of Nb leading to its embrittlement. Ti and Hf are the only elements that do not increase the BDTT in Nb. Recent results have indicated that Ti is beneficial to improve the fracture toughness of solid-solution alloys by reducing Peirels–Nabarro (P–N) barrier energy, while Al and Cr are undesirable in the enhancement of fracture toughness and tensile ductility [10]. However, the addition of Cr and Al is indispensable in Nb for their positive effects on oxidation resistance [11,12].

Recently, Nb–Si–Ti–Cr system alloy is widely studied in the research field of Nb–Si based alloys [13–17]. As mentioned previously, Nb–Si based alloy consisted of Nb_{SS} and Nb–silicide. The purpose of the addition of Si is to form Nb_3Si and/or α, β, γ-Nb_5Si_3, and Si is also one of the solid solution elements in Nb_{SS}. According to the Nb–Si binary phase diagram, the maximum solid solubility of Si in Nb is merely 3.5%. Bewlay et al. have reported that the solubility of Si in Nb was approximately 1% [18]. From studies of Tsakiropoulos et al., the content of Si was 1–2.7% in Nb_{SS} for arc-cast Nb–Si alloys, while it reduced to 0–1.2% after heat treatment [19–21]. However, the influence of minor amounts of Si on microstructure and mechanical properties of Nb_{SS} is unclear. Therefore, the understanding of effects of Si on Nb solid solution is crucial for alloy designing. In our previous work, a Nb–12Si–24Ti–10Cr–2Al–2Hf alloy prepared by direction solidification plus heat treatment showed superior performance [22]. The average chemical composition of NbSS in the alloy is Nb–0.84Si–27.63Ti–12.92Cr–2.07Al–1.12Hf detected by energy-dispersive spectrometer; thus Nb–27.63Ti–12.92Cr–2.07Al–1.12Hf was chosen as the base alloy. 0%, 0.5%, 1% and 2% Si were added to the base alloy to investigate the mechanism of the effect of minor Si content (0–2%) on Nb_{SS}.

* Corresponding author. Tel.: +86 10 82316958; fax: +86 10 82338598.
E-mail addresses: kongbin@buaa.edu.cn (B. Kong), jialina@buaa.edu.cn (L. Jia), sulinfen@mse.buaa.edu.cn (L. Su), guankai@mse.buaa.edu.cn (K. Guan), wengjf@mse.buaa.edu.cn (J. Weng), zhanghu@buaa.edu.cn (H. Zhang).

http://dx.doi.org/10.1016/j.msea.2015.04.096
0921-5093/© 2015 Published by Elsevier B.V.

2. Experimental procedures

In this work, Nb-based solid solution alloy ingots were prepared by vacuum non-consumable arc casting in argon atmosphere with nominal compositions of Nb–(0/0.5/1/2)Si–27.63Ti–12.92Cr–2.07Al–1.12Hf. Each master alloy button ingot was remelted four times to ensure chemical homogeneity. The arc-casting samples were marked as AC0, AC0.5, AC1, and AC2 based on the difference of Si content. Half of the buttons were then heat treated at 1425 °C for 10 h in a high vacuum heat treatment furnace with proper argon atmosphere. The heat-treated samples were marked as HT0, HT0.5, HT1 and HT2, corresponding to the original AC specimens.

Samples for microstructure observations and U-notched three-point bending tests were prepared by electro-discharge machining. Backscatter electron (BSE) images of microstructures of alloys were taken by Electron probe micro-analyzer (EPMA; Model JXA-8230) and scanning electron microscope (SEM; JSM-7500; Quanta 200F). Energy-dispersive spectrometer (EDS; Oxford INCAPentaFET-x3) was used to analyze the chemical composition. Image-Pro Plus software was used to quantitatively analyze the primary Nb_{SS} dendrite arm spacing (PDAS), the Nb_{SS} grain size and the volume fraction of phases. The results were the average of at least 6 individual measurements. Fracture toughness test using the single-edge U-notched three-point bending specimens with dimensions of $30 \times 6 \times 3\ mm^3$ was conducted on an SAN hydraulic servo machine with a compaction head loading rate of 0.1 mm/min at room temperature. Secondary electron (SE) images of fracture surfaces of three-point bending samples were taken by scanning electron microscope (SEM; JEOL 6010).

3. Results

3.1. Microstructures of arc casting alloys

Fig. 1 shows the microstructures of AC samples. Three regions with white, gray and dark contrast are observed clearly. EDS results (Table 1) show that the regions with white contrast are coarse Nb_{SS} dendrites that predominate in the microstructure of AC samples. The regions with gray contrast existing at the boundary of Nb_{SS} dendrites are Ti-rich Nb_{SS}, containing less Nb but more Ti and Cr as compared to Nb_{SS} dendrites. The regions with dark contrast located in the center of Ti-rich Nb_{SS} are interdendritic precipitates.

As illustrated in high magnification images (Fig. 2), the structure of interdendritic precipitates (regions with dark contrast) in arc-casting alloys is displayed. With the increase of Si content, more precipitates could be observed. These precipitates consist of Cr_2Nb Laves phase and silicides including $(Nb,Ti)_3Si$ and γ-$(Nb,Ti)_5Si_3$ (except in AC0 alloy), which are confirmed by TEM. The selected-area diffraction patterns (SADPs) taken from different phases are shown in Fig. 3. Ti-rich Nb_{SS} phase is a body centered cubic structure (Fig. 3(c)), and Cr_2Nb phase is a $MnZn_2$ type hexagonal C14 structure (Fig. 3(d)). $(Nb,Ti)_3Si$ phase possesses a PTi_3 type tetragonal structure (Fig. 3(e)), and $(Nb,Ti)_5Si_3$ phase is a Mn_5Si_3 type hexagonal $D8_8$ structure (Fig. 3(f)), which is identified as γ-$(Nb,Ti)_5Si_3$.

As shown in Fig. 4, in AC alloys, the primary Nb_{SS} dendrite arm spacing (PDAS) decreases with the increase of Si content indicating that Nb_{SS} dendrites are refined gradually. It could be deduced that with the increase of Si content, more silicides and Cr_2Nb Laves phases form in the interdendritic regions due to elements segregation. The further growth of Nb_{SS} dendrites is restrained by interdendritic precipitates leading to the decrease of PDAS.

According to the phase compositions and morphologies, the solidification path could be deduced. The primary phase is Nb_{SS} dendrites so that solidification path is $L \rightarrow Nb_{SS} + L_1$. As the solidification progresses, low melting temperature elements such as Ti and Cr become enriched in the residual liquid (L_1). Multi-phase eutectics crystallize in the interdendritic region as liquid (L_1) reaches the eutectic composition, and the eutectic reaction $L_1 \rightarrow$ Eutectic (Ti-rich $Nb_{SS} + Cr_2Nb + (Nb,Ti)_3Si + \gamma$-$(Nb,Ti)_5Si_3$) + Ti-rich Nb_{SS} may occur.

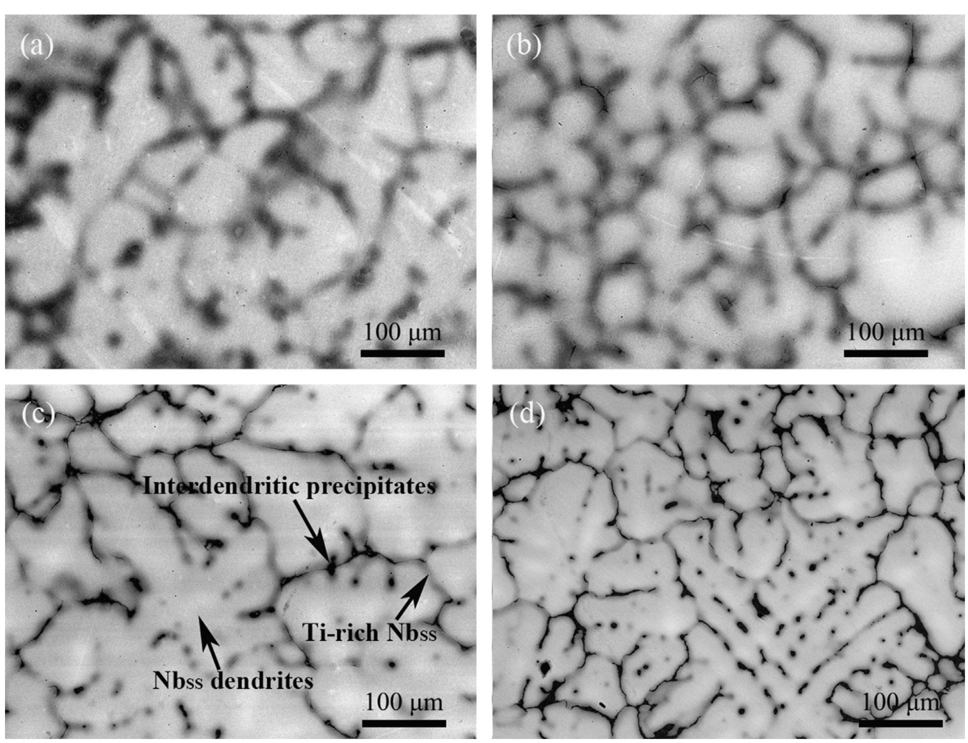

Fig. 1. BSE images of microstructures of AC alloys: (a) AC0; (b) AC0.5; (c) AC1; (d) AC2.